Phase coupling in Langmuir wave packets: Evidence of four wave interactions in solar type III radio bursts

G. Thejappa,[1] R. J. MacDowall,[2] and M. Bergamo[1]

Received 18 January 2012; revised 8 February 2012; accepted 9 February 2012; published 7 March 2012.

[1] It is reported that one of the Langmuir wave packets in a type III solar radio burst is observed as a localized field structure with a short duration ~3.2 ms and high intensity exceeding the strong turbulence thresholds. The peak intensity and short time scale well satisfy the criterion for the observed wave packet to be the collapsing Langmuir envelope soliton. The spectrum of this wave packet contains a resonant peak at the local electron plasma frequency, f_{pe}, a Stokes peak at a frequency slightly lower than f_{pe}, anti-Stokes peak at a frequency slightly higher than f_{pe}, and a low frequency enhancement below a few hundred Hz, which satisfy the frequency and wave number resonance conditions of the oscillating two stream instability (OTSI) type of four wave interaction. Here, for the first time, we apply the trispectral analysis technique, and show that the spectral components of this wave packet, namely, the beam-generated Langmuir wave, Stokes and anti-Stokes modes are coupled to each other with a high degree of phase coherency (high tricoherence). This conclusively shows that the observed characteristics of the wave packet provide evidence for the OTSI. **Citation:** Thejappa, G., R. J. MacDowall, and M. Bergamo (2012), Phase coupling in Langmuir wave packets: Evidence of four wave interactions in solar type III radio bursts, *Geophys. Res. Lett.*, *39*, L05103, doi:10.1029/2012GL051017.

1. Introduction

[2] The characteristic feature of solar type III radio bursts is the fast negative frequency drift from hundreds of MHz to tens of kHz. *Ginzburg and Zheleznyakov* [1958] were the first to propose a two step process for the production of these bursts: (1) excitation of high levels of Langmuir waves at the local electron plasma frequency $f_{pe} = 9n_e^{1/2}$ by flare accelerated electron beams through bump-on-tail instability (n_e is the electron density in m^{-3}), and (2) subsequent conversion of these Langmuir waves into radio emissions at f_{pe} and $2f_{pe}$. This hypothesis, known as the plasma hypothesis, has been confirmed by the in situ detection of electron beams [*Lin et al.*, 1973, 1986] as well as Langmuir waves [*Gurnett and Anderson*, 1976] in type III burst source regions. However, the question, how does the electron beam preserve its bump-on-tail distribution over distances of 1 AU and more against quasi-linear relaxation (Sturrock's dilemma [*Sturrock*, 1964]), remains unanswered. Here, one should note that Sturrock did not consider the effects of re-acceleration of beam particles by Langmuir waves. For example, by treating the wave particle interaction along the beam path self-consistently, some authors [*Zaitsev et al.*, 1972; *Escande and de Genouillac*, 1978] claim that the beam can survive large distances of the order of 1 AU and more.

[3] Currently, it is believed that some nonlinear process, which can pump the Langmuir waves out of resonance with the beam faster than the quasi-relaxation time is probably responsible for beam stabilization. The induced scattering off ion clouds, whose resonance version is the electrostatic decay (ESD) of initial Langmuir wave into a daughter Langmuir wave and an ion sound wave when $T_e > T_i$ (T_e and T_i are the electron and ion temperatures, respectively) is suggested as one such mechanism [*Kaplan and Tsytovich*, 1968]. Although some signatures of ESD are detected in type III sources [*Lin et al.*, 1986; *Gurnett et al.*, 1993; *Hospodarsky and Gurnett*, 1995; *Thejappa and MacDowall*, 1998; *Thejappa et al.*, 2003; *Henri et al.*, 2009], the time scale appears to be too long to prevent the plateau formation [*Zheleznyakov and Zaitsev*, 1970]. Some authors suggested that the strong turbulence processes, namely, the four-wave interactions called the OTSI [*Papadopoulos et al.*, 1974; *Smith et al.*, 1979; *Goldstein et al.*, 1979], and related soliton formation and spatial collapse [*Zakharov*, 1972; *Nicholson et al.*, 1978] are more effective in stabilizing the electron beam. The OTSI excites a low frequency ion sound wave, which can beat with two of the beam-excited Langmuir waves and produce down-shifted and up-shifted side bands. The spatial collapse, on the other hand, occurs due to intensification of the Langmuir wave packet in the self generated density cavity. Although some signatures of the strong turbulence processes in Jupiter's foreshock [*Gurnett et al.*, 1981], solar wind [*Kellogg et al.*, 1992], and source regions of type III bursts [*Thejappa et al.*, 1993; *Thejappa and MacDowall*, 1998; *Thejappa et al.*, 1999; *Thejappa and MacDowall*, 2004] have been reported, in these cases, high intensities which are well above strong turbulence thresholds and the sideband spectral structures were not observed simultaneously.

[4] *Thejappa et al.* [2012] have reported the high time resolution observations of a Langmuir wave packet associated with a type III radio burst. This wave packet is characterized by (1) side band spectral structures as well as low frequency enhancement which satisfy the frequency and wave number matching rules of OTSI, and (2) peak intensity which satisfies not only the threshold condition of OTSI, but also the criterion for the observed wave packet to be the collapsing envelope soliton. In this study, for the first time, we apply the trispectral analysis on this Langmuir wave packet, and show that its spectral components, namely, the

[1]Department of Astronomy, University of Maryland, College Park, Maryland, USA.
[2]NASA Goddard Space Flight Center, Greenbelt, Maryland, USA.

0094-8276/12/2012GL051017

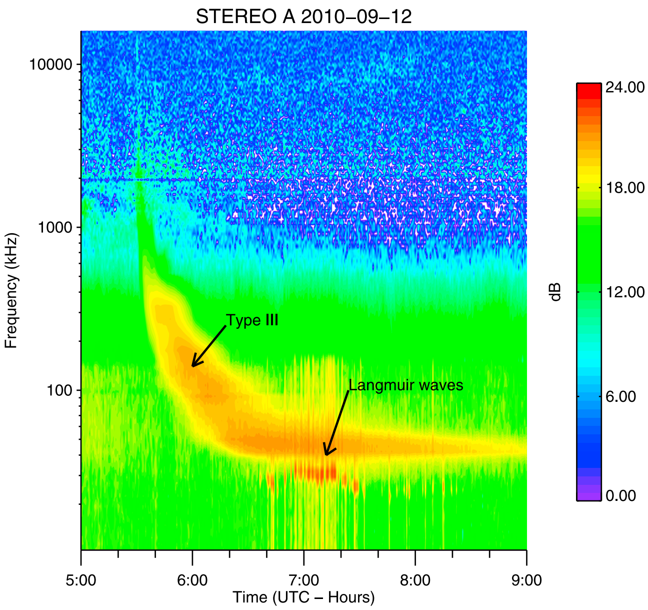

Figure 1. Dynamic spectrum of a local type III radio burst (fast drifting emission from ~5 MHz down to ~30 kHz) and associated Langmuir waves (non-drifting emissions in the frequency interval 27-32 kHz).

beam-generated Langmuir wave, Stokes and anti-Stokes modes are coupled to each other with a high degree of phase coherency (high tricoherence). This conclusively shows that these observations provide evidence for the OTSI as correctly concluded by *Thejappa et al.* [2012]. In section 2, we review the observations, and in sections 3 and 4,we present the trispectral analysis and conclusions, respectively.

2. Review of Observations

[5] Figure 1 shows the STEREO/WAVES [*Bougeret et al.*, 2008] observations of a local type III burst, drifting fast from ~5 MHz to the local electron plasma frequency, $f_{pe} \sim 30$ kHz, and non-drifting Langmuir wave emissions in the 27–32 kHz interval. The Time Domain Sampler (TDS) [*Kellogg et al.*, 2009] of the SWAVES experiment, which samples the A/C electric field from 3 orthogonal antennas has resolved these Langmuir waves into intense waveforms. Each of these waveforms contains 16384 samples with an acquisition rate of 250,000 samples per second (a time step of 4 μs for a total duration of 65 ms). Figure 2 shows the most intense wave packet captured by the E_x antenna, which is characterized by the peak electric field strength E_L of 56.5 mVm^{-1} and $\frac{1}{e}$-power duration τ of ~3.2 ms. Since the E_y, E_z and E_{x-y} signals are weaker and show the same general features as the E_x signal, *Thejappa et al.* [2012] analyzed only the E_x signal, and justified one-dimensional treatment by assuming that these Langmuir wave fields are probably aligned along the ambient magnetic field. Figure 3 shows the spectral characteristics of this wave packet: (a) the total spectrum extending from 0 to 65 kHz, (b) the narrow spectrum, containing an intense peak (L) at $f_{pe} \sim 30$ kHz, corresponding to $n_e \sim 1.1 \times 10^7$ m^{-3}, a Stokes peak (D) at ~29.54 kHz and an anti-Stokes peak (U) at ~30.41 kHz, and (c) the low frequency spectrum, containing a clear ion-sound wave associated enhancement below 450 Hz. The STEREO/PLASTIC experiment [*Galvin et al.*, 2008] has measured the solar wind speed v_{sw} as ~450 kms^{-1}. The

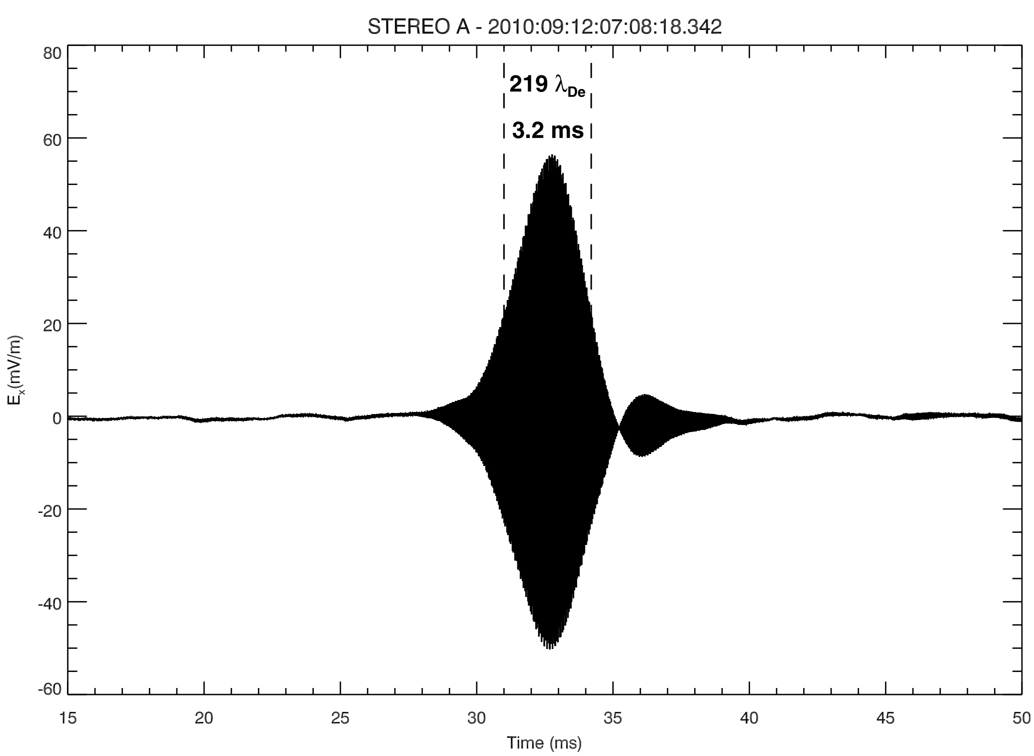

Figure 2. The Langmuir wave packet observed by the Time Domain Sampler (TDS) during the type III event of Figure 1. The $\frac{1}{e}$ power duration of 3.2 ms which is equivalent to the spatial scale of 219λ_{De} is also shown.

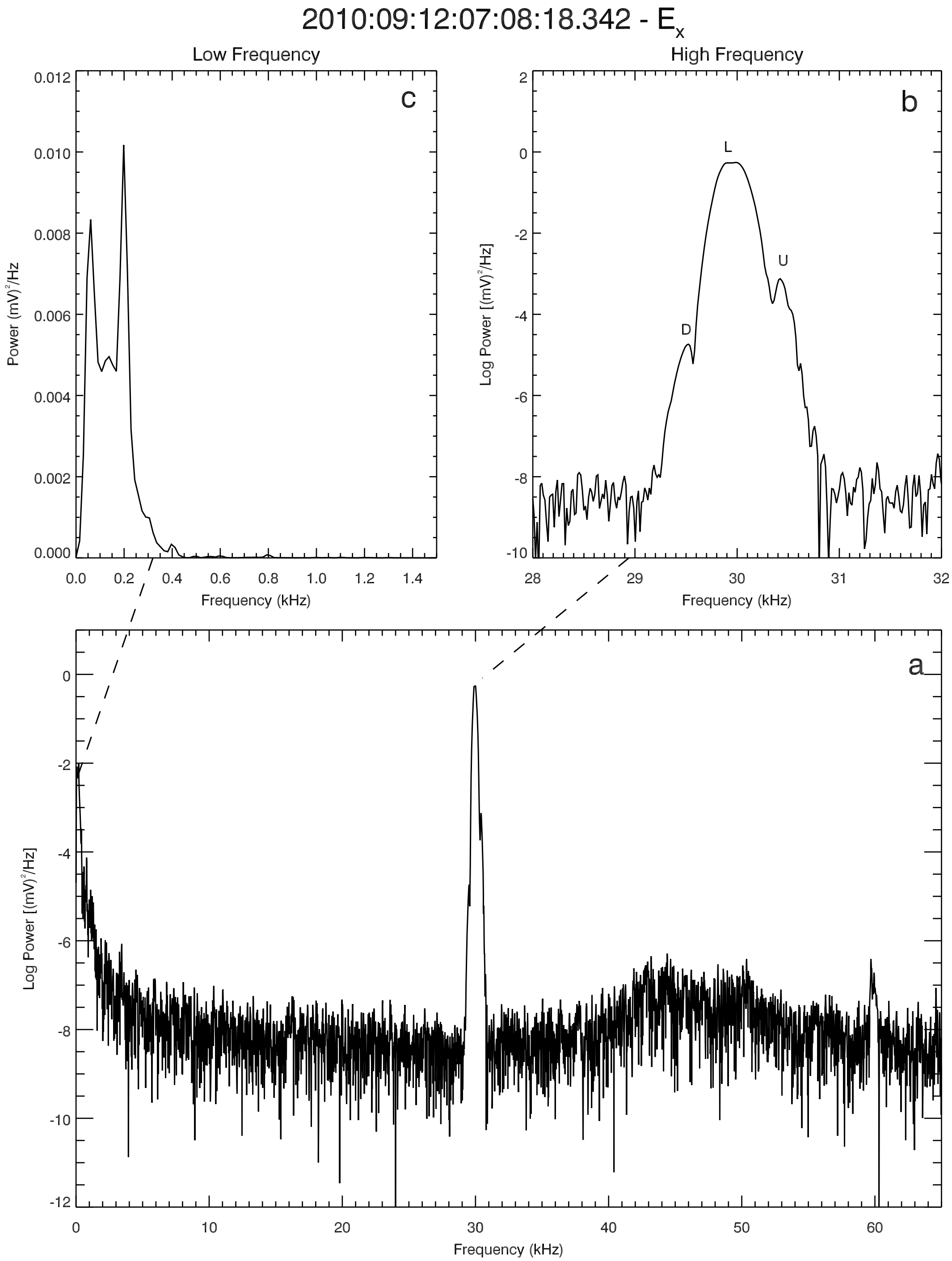

Figure 3. (a) The spectrum of the TDS event from 0 to 65 kHz, (b) the narrow spectrum around $f \sim f_{pe} \sim 30$ kHz, where the L, D, and U refer to the beam excited Langmuir wave, Stokes peak at ~29.54 kHz, and anti-Stokes peak at ~30.41 kHz, respectively, and (c) the low frequency spectrum which shows an enhancement below 450 Hz corresponding probably to ion-sound waves.

electron temperature T_e during this event is assumed to be $\sim 10^5$ K. Assuming that the type III electrons propagate along the Parker's spiral field lines, a frequency drift curve is fitted to the dynamic spectrum. This yielded the beam speed v_b of $\sim 0.22c$ for the Radio Astronomy Explorer (RAE) density model [*Fainberg and Stone*, 1971] (c is the velocity of light). Since, the pitch angle scattering is known to increase the path length of electron beams by a factor of α = 1.3 to 1.7 [*Alvarez et al.*, 1975; *Lin et al.*, 1973], the beam speeds v_b and the wave numbers of Langmuir waves $k_L = \frac{\omega_{pe}}{v_b}$ are corrected accordingly to range from $\sim 0.29c$ to $\sim 0.37c$, and from $\sim 2.2 \times 10^{-3}$ m^{-1} to $\sim 1.7 \times 10^{-3}$ m^{-1}, respectively. The observed quantities yielded: (1) Debye length, $\lambda_{De} = 69 T_e^{1/2} n_e^{-1/2} \sim 6.6$ m, and (2) normalized peak energy density $\frac{W_L}{n_e T_e} = \frac{\varepsilon_0 E_L^2}{2 n_e T_e} \sim 10^{-3}$, and (3) the $\frac{1}{e}$-power spatial scale of the wave packet $S \sim \tau v_{sw} \sim 219 \lambda_{De}$.

[6] The threshold for the OTSI [*Zakharov*, 1972] $\frac{W_L}{n_e T_e} > (k_L \lambda_{De})^2$ is easily satisfied in this case, since $\frac{W_L}{n_e T_e} \sim 10^{-3}$ and $(k_L \lambda_{De})^2$ ranges from $\sim 1.3 \times 10^{-4}$ to $\sim 2.1 \times 10^{-4}$. The wave packet also satisfies the criterion of a collapsing envelope soliton [*Thornhill and ter Haar*, 1978] $\frac{W_L}{n_e T_e} \geq (\Delta k \lambda_{De})^2$, ($\Delta k = \frac{2\pi}{S}$ is the wave number characteristic of the envelope), since the observed $\frac{W_L}{n_e T_e} \sim 10^{-3}$ is greater than $(\Delta k \lambda_{De})^2 \sim 8 \times 10^{-4}$ estimated for the spatial scale S of $\sim 219\lambda_{De}$.

[7] The observations of a strong Langmuir wave peak with upper and lower sidebands, together with low frequency enhancement were interpreted in terms of OTSI, in which, the beam driven Langmuir wave is the pump wave, and the sidebands and low frequency waves are the non-linearly excited daughter waves. The frequency matching condition $2f_L = f_D + f_U$ is easily satisfied, since the frequency shifts Δf of the down-shifted and up-shifted side bands are symmetric with respect to the Langmuir wave pump, being $\sim$442.5 Hz and $\sim$427 Hz, respectively, which are also in good agreement with the frequencies of the ion sound waves of <450 Hz. Using the expression for the Doppler's shift $\Delta f = \frac{v_{sw}}{2\pi\lambda_{De}}(k\lambda_{De})\cos\theta$, the wave numbers $k\lambda_{De}$ can be estimated as ~ -0.04 and ~ 0.04 for Δf of $\sim$442.5 Hz and 427 Hz corresponding to the Stokes and anti-Stokes modes, respectively. Here, θ is the angle between $\vec{k}$ and $\vec{v}_{sw}$; $\theta = 0$ and $\theta = \pi$ correspond to the anti-Stokes and Stokes modes propagating away from and toward the Sun, respectively. This suggests that the beam excited Langmuir waves with $k_L \lambda_{De} \sim 10^{-2}$ are pumped into those of forward and backward propagating daughter waves with higher wave numbers. Similarly, using the expression for the Doppler shift, $q = \frac{2\pi\Omega}{v_{sw}}$, the wave numbers of the ion sound waves $q\lambda_{De}$ can be estimated as $\simeq 0.042$ for $\Omega = 450$ Hz and $v_{sw} = 450$ kms^{-1}, which are comparable to those of the sideband emissions. Thus, the matching condition $\vec{k} = \vec{k}_{\mathrm{L}} \pm \vec{q}$ is reasonably satisfied, yielding $|\vec{k}| \simeq |\vec{q}|$, since k_L is three to four times less than q.

[8] In the present case, the inequalities $k_L \leq (\frac{m_e}{m_i})^{1/2} k_D$ and $\frac{W_L}{n_e T_e} > \frac{m_e}{m_i}$ are easily satisfied, indicating that the wave packet is in the supersonic modulational instability regime as referred by *Zakharov et al.* [1985]. Here $m_{e,\,i}$ are the electron and ion masses, respectively, and $k_D = \frac{1}{\lambda_{De}}$. The growth rate of the OTSI $\frac{\Gamma}{\omega_{pe}} \sim (\frac{m_e}{3m_i} \frac{W_L}{4n_e T_e})^{1/2}$ is $\sim 4.3 \times 10^{-4}$, whereas, the bandwidth $\frac{\Delta\omega}{\omega_{pe}} = 3(k_L \lambda_{De})^2 \frac{\Delta k_L}{k_L}$ is $\sim 3 \times 10^{-6}$. Here, the spectral width $\frac{\Delta k_L}{k_L} = \frac{\Delta v_b}{v_b} \frac{\ln 2}{2N}$ [*Lin et al.*, 1986; *Benz*, 2002] is estimated for the velocity spread of the beam $\Delta v_b \sim 0.1 v_b$ and the linear growth times N before the onset of OTSI of $\sim$9. Thus, the growth rate is much larger than the bandwidth, which indicates that the observed wave packet is monochromatic enough for excitation of OTSI.

3. Trispectral Analysis

[9] In the power spectrum estimation, the waveform is treated as a superposition of statistically uncorrelated harmonic components, and the phase relations between the spectral components are suppressed. To extract the information regarding the presence of nonlinearities, one has to use the higher order spectra, defined in terms of the higher order moments or cumulants of the data. The third-order spectrum, commonly referred to as the bispectrum decomposes the signal's third moment over frequency. Since it is related to the skewness of a signal, it is usually used to detect the asymmetric non-linearities, such as the electrostatic decay [*Henri et al.*, 2009; *Balikhin et al.*, 2001; *Walker et al.*, 2003] and harmonic generation [*Bale et al.*, 1996]. The amplitude of the bispectrum at the bifrequency (f_k, f_l) measures the amount of coupling between the frequencies, f_k, f_l and f_{k+l}.

[10] The fourth-order spectrum is referred to as the trispectrum. It can be viewed as the decomposition of the signal's kurtosis over frequency. If the signal is unskewed and contains information about a symmetric process, such as the OTSI type of four wave interaction, it can be extracted using the trispectral analysis. The trispectral method has been developed [*Kravtchenko-Berejnoi et al.*, 1995a] and applied to synthetic [*Kravtchenko-Berejnoi et al.*, 1995b; *Lefeuvre et al.*, 1995] and to simulated data [*Soucek et al.*, 2003]. The trispectral analysis can detect the phase relationships among four Fourier components, which is the key information regarding four-wave interaction. In OTSI, the sidebands interact with the strong beam excited Langmuir waves satisfying the matching rules for wave numbers, frequencies and phases, simultaneously. For the OTSI type of four-wave interaction, the cumulant based trispectrum is given by [*Kravtchenko-Berejnoi et al.*, 1995a]

$$T(1,2,3) = E[X_1 X_2 X_3^* X_4^*] - N(1,2,3,4), \quad (1)$$

where X_1, X_2, X_3 and X_4 are the complex Fourier components of the signal corresponding to frequencies f_1, f_2, f_3 and f_4, $N(1, 2, 3, 4) = E[X_1 X_2]E[X_3^* X_4^*] + E[X_1 X_3^*]E[X_2 X_4^*] + E[X_1 X_4^*]E[X_2 X_3^*]$, $f_4 = f_1 + f_2 - f_3$, and $E[]$ is the expectation operator. The tricoherence, which is the normalized trispectrum is more useful, because it eliminates the dependence of trispectrum on the amplitude of the signals. The expressions for cumulant based square tricoherence function can be written as [*Kravtchenko-Berejnoi et al.*, 1995a]:

$$t^2(1,2,3) = \frac{|T(1,2,3)|^2}{(E[|X_1 X_2 X_3^* X_4^*|] + |N(1,2,3,4)|)^2}. \quad (2)$$

A unit value for the tricoherence indicates perfect coupling, a zero value indicates no coupling, and any value between zero and one indicates partial coupling. The tricoherence quantifies the fraction of the total product of powers at the frequency quartet (f_1, f_2, f_3, $f_1 + f_2 - f_3$), that is owing to cubicly phase-coupled modes. The tricoherence is zero for a Gaussian process. Even for a Gaussian process, due to statistical fluctuations, the estimate of the tricoherence from a finite data record will not be zero. Therefore, the method of periodograms is used to estimate the trispectrum and tricoherence. This involves the division of the data record into M segments; an appropriate window is applied to each segment to reduce leakage; the trispectrum as well as tricoherence are computed for each segment by using the DFT; finally, the trispectrum is averaged across segments in order to reduce the variance of the estimator. As seen from equation (1), the trispectrum estimator is symmetric with respect to permutations of its arguments f_1, f_2 and f_3. The principal domain for the interaction of the type $f_1 + f_2 = f_3 + f_4$ is determined as [*Kravtchenko-Berejnoi et al.*, 1995a]

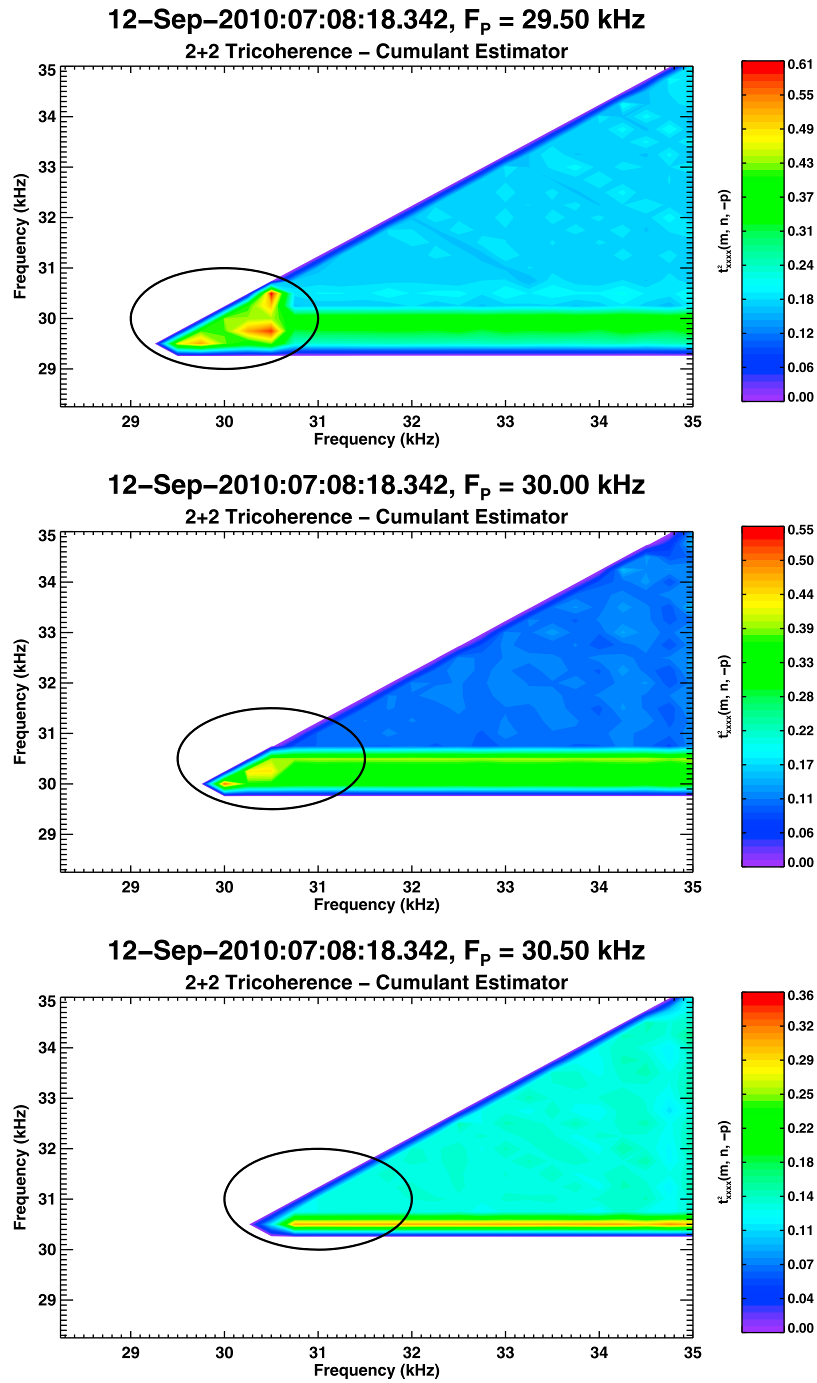

Figure 4. The cross-sections of the tricoherence spectrum of the TDS event of Figure 2 at Stokes, beam-excited Langmuir and anti-Stokes frequencies (top to bottom), respectively.

$0 \le f_1 \le f_N$, $0 \le f_2 \le f_1$, $0 \le f_3 \le f_2$, and $f_3 \le f_1 + f_2 - f_3 \le f_N$, where f_N is the Nyquist frequency.

[11] In this study, we have used the segment length N = 1000 (0.004 s), number of segments M = 16 and Hamming window, and calculated the tricoherence spectrum as a function of three frequencies. Since it is difficult to visualize the results in such a 3-D space, we have fixed one of its frequencies and displayed the results in two dimensions. We have made the cross-sections of the tricoherence spectrum at frequencies f_D = 29.5 kHz, f_L = 30 kHz and f_U = 30.5 kHz, corresponding to the Stokes, beam-excited Langmuir, and anti-Stokes modes, respectively. In Figure 4, we present these cross sections. The cross-section of the tricoherence spectrum at f_D = 29.5 kHz(top panel) shows: (1) a peak at (29.5 kHz, 29.5 kHz, 29.5 kHz); this is due to self-dependence and is of no interest, (2) a second peak at (30.5 kHz, 30 kHz, 29.5 kHz), which is due to the phase relation $2\phi_L = \phi_D + \phi_U$, where ϕ_L, ϕ_D and ϕ_U are the phases of the beam-excited Langmuir, Stokes and anti-Stokes modes, respectively; the maximum tricoherence $t^2 \sim 0.53$ in this case, and (3) a third peak at (30.5 kHz, 30.5 kHz, 29.5 kHz); this appears to be due to the interaction of the sidebands themselves, and it is of no interest in the present case. The cross-section of the tricoherence spectrum at

f_L = 30 kHz (second panel) shows (1) a peak at (30 kHz, 30 kHz, 30 kHz), which is due to self-dependence, and (2) a second peak at (30 kHz, 30.5 kHz, 30 kHz), which is due to the phase relation $2\phi_L = \phi_D + \phi_U$; in this case, the maximum $t^2 \sim 0.5$. The tricoherence cross-section at f_U = 30.5 kHz (bottom panel) does not show any peaks. Thus, the significant tricoherences corresponding to $2\phi_L = \phi_D + \phi_U$ in the cross-sections of the tricoherence spectrum at Stokes and beam-excited Langmuir wave frequencies provide evidence for the OTSI type of four-wave interaction.

4. Conclusions

[12] *Thejappa et al.* [2012] had reported the high time resolution observations of a very coherent and intense Langmuir wave packet in the source region of a local type III radio burst. This wave packet is characterized by (1) a spectrum containing (a) a resonant peak at the local electron plasma frequency, f_{pe}, (b) Stokes peak at a frequency slightly lower than f_{pe}, (c) anti-Stokes peak at a frequency slightly higher than f_{pe}, and (d) low frequency enhancement corresponding to ion sound fluctuations; the frequencies and wave numbers of these spectral components satisfy the resonance conditions of oscillating two stream instability (OTSI), (2) peak intensity, which is well above the threshold for strong turbulence processes, and (3) short time scale of a few ms. These observations were interpreted in terms of OTSI. In this study, for the first time, applying the trispectral analysis on this Langmuir wave packet, it is shown that the spectral components of the wave packet are coupled to each other with a high degree of phase coherency (high tricoherence), which provides crucial support for the interpretation of these observations in terms of OTSI.

[13] **Acknowledgments.** The research of T. G. is supported by the NASA grants NNX08AO02G and NNX09AB19G. The SWAVES instruments include contributions from the Observatoire of Paris, University of Minnesota, University of California, Berkeley, and NASA/GSFC. We thank M. J. Reiner for calculating the electron beam speed. We also thank the referees for very constructive comments and helpful suggestions.

[14] The Editor thanks Donald Gurnett and an anonymous reviewer for their assistance in evaluating this paper.

References

Alvarez, H., R. P. Lin, and S. J. Bame (1975), Fast solar electrons, interplanetary plasma and km-wave type-III radio bursts observed from the IMP-6 spacecraft, *Sol. Phys.*, *44*, 485.

Bale, S. D., D. Burgess, P. J. Kellogg, K. Goetz, R. L. Howard, and S. J. Monson (1996), Phase coupling in Langmuir wave packets: Possible evidence of three-wave interactions in the upstream solar wind, *Geophys. Res. Lett.*, *23*, 109.

Balikhin, M. A., I. Bates, and S. Walker (2001), identification of linear and nonlinear processes in space plasma turbulence data, *Adv. Space Res.*, *28*, 787.

Benz, A. O. (2002), *Plasma Astrophysics: Kinetic Processes in Solar and Stellar Coronae*, *Astrophys. Space Sci. Libr.*, vol. 279, Kluwer Acad., Dordrecht, Netherlands.

Bougeret, J.-L., et al. (2008), S/WAVES: The radio and plasma wave investigation on the STEREO Mission, *Space Sci. Rev.*, *136*, 487.

Escande, D. F., and G. V. de Genouillac (1978), Electron burst relaxation in a fluctuating plasma, *Astron. Astrophys.*, *68*, 405.

Fainberg, J., and R. G. Stone (1971), Type III solar radio burst storms observed at low frequencies, *Sol. Phys.*, *17*, 392.

Galvin, A. B., et al. (2008), The Plasma and Suprathermal Ion Composition (PLASTIC) investigation on the STEREO observatories, *Space Sci. Rev.*, *136*, 437.

Ginzburg, V. L., and V. V. Zheleznyakov (1958), On the possible mechanisms of sporadic solar radio emission (radiation in an isotropic plasma), *Sov. Astron.*, *2*, 623.

Goldstein, M. L., R. A. Smith, and K. Papadopoulos (1979), Nonlinear stability of solar type III radio bursts. II. Application to observations near 1 AU, *Astrophys. J.*, *234*, 683.

Gurnett, D. A., and R. R. Anderson (1976), Electron plasma oscillations associated with type III radio bursts, *Science*, *194*, 1159.

Gurnett, D. A., J. E. Maggs, D. L. Gallagher, W. S. Kurth, and F. L. Scarf (1981), Parametric interaction and spatial collapse of beam-driven Langmuir waves in the solar wind, *J. Geophys. Res.*, *86*, 8833.

Gurnett, D. A., G. B. Hospodarsky, W. S. Kurth, D. J. Williams, and S. J. Bolton (1993), Fine structure of Langmuir waves produced by a solar electron event, *J. Geophys. Res.*, *98*, 5631.

Henri, P., C. Briand, A. Mangeney, S. D. Bale, F. Califano, K. Goetz, and M. Kaiser (2009), Evidence for wave coupling in type III emissions, *J. Geophys. Res.*, *114*, A03103, doi:10.1029/2008JA013738.

Hospodarsky, G. B., and D. A. Gurnett (1995), Beat-type Langmuir wave emissions associated with a type III solar radio burst: Evidence of parametric decay, *Geophys. Res. Lett.*, *22*, 1161.

Kaplan, S. A., and V. N. Tsytovich (1968), Radio emission from beams of fast particles under cosmic conditions, *Sov. Astron.*, *11*, 956.

Kellogg, P. J., K. Goetz, R. L. Howard, and S. J. Monson (1992), Evidence for Langmuir wave collapse in the interplanetary plasma, *Geophys. Res. Lett.*, *19*, 1303.

Kellogg, P. J., K. Goetz, S. J. Monson, S. D. Bale, M. J. Reiner, and M. Maksimovic (2009), Plasma wave measurements with STEREO S/WAVES: Calibration, potential model, and preliminary results, *J. Geophys. Res.*, *114*, A02107, doi:10.1029/2008JA013566.

Kravtchenko-Berejnoi, V., F. Lefeuvre, L. V. Krasnoselskikh, and D. Lagoutte (1995a), On the use of tricoherent analysis to detect non-linear wave-wave interactions, *Signal Process.*, *42*, 291.

Kravtchenko-Berejnoi, V., V. Krasnoselskikh, D. Mourenas, and F. Lefeuvre (1995b), Higher-order spectra and analysis of a non-linear dynamic model, in *Proceedings of the Cluster Workshops: Data Analysis Tools, Braunschweig, Germany, 28–30 September 1994*, *Eur. Space Agency Spec. Publ.*, *ESA SP-371*, 61.

Lefeuvre, F., V. Kravtchenko-Berejnoi, and D. Lagoutte (1995), Higher-order spectra and analysis of a non-linear dynamic model, in *Proceedings of the Cluster Workshops: Data Analysis Tools, Braunschweig, Germany, 28–30 September 1994*, *Eur. Space Agency Spec. Publ.*, *ESA SP-371*, 51.

Lin, R. P., L. G. Evan, and J. Fainberg (1973), Simultaneous observations of fast solar electrons and type III radio burst emission near 1 AU, *Astrophys. Lett.*, *14*, 191.

Lin, R. P., W. K. Levedahl, W. Lotko, D. A. Gurnett, and F. L. Scarf (1986), Evidence for nonlinear wave-wave interactions in solar type III radio bursts, *Astrophys. J.*, *308*, 954.

Nicholson, D. R., M. V. Goldman, P. Hoyang, and J. C. Weatherall (1978), Nonlinear Langmuir waves during type III solar radio bursts, *Astrophys. J.*, *223*, 605.

Papadopoulos, K., M. L. Goldstein, and R. A. Smith, (1974), Stabilization of electron streams in type III solar radio bursts, *Astrophys. J.*, *190*, 175.

Smith, R. A., M. L. Goldstein, and K. Papadopoulos (1979), Nonlinear stability of solar type III radio bursts. I. Theory, *Astrophys. J.*, *234*, 348.

Soucek, J., T. Dudok de Wit, V. Krasnoselskikh, and A. Volokitin (2003), Statistical analysis of nonlinear wave interactions in simulated Langmuir turbulence data, *Ann. Geophys.*, *21*, 681.

Sturrock, P. A. (1964), Type III solar radio bursts, in *Proceedings of AAS-NASA Symposium on the Physics of Solar Flares*, *NASA SP*, vol. 50, edited by W. N. Hess, p. 357, Sci. and Tech. Inf. Div., Washington, D. C.

Thejappa, G., D. Lengyel-Frey, R. G. Stone, and M. L. Goldstein (1993), Evaluation of emission mechanisms at ω_{pe} using Ulysses observations of type III bursts, *Astrophys. J.*, *416*, 831.

Thejappa, G., and R. J. MacDowall (1998), Evidence for strong and weak turbulence processes in the source region of a local type III radio burst, *Astrohpys. J.*, *498*, 465.

Thejappa, G., and R. J. MacDowall (2004), High frequency ion sound waves associated with Langmuir waves in type III radio burst source regions, *Nonlinear Processes Geophys.*, *11*, 411.

Thejappa, G., M. L. Goldstein, R. J. MacDowall, K. Papadopoulos, and R. G. Stone (1999), Evidence for Langmuir envelope solitons in solar type III burst source regions, *J. Geophys. Res.*, *104*, 28,279.

Thejappa, G., R. J. MacDowall, E. E. Scime, and J. E. Littleton (2003), Evidence for electrostatic decay in the solar wind at 5.2 AU, *J. Geophys. Res.*, *108*(A3), 1139, doi:10.1029/2002JA009290.

Thejappa, G., R. J. MacDowall, M. Bergamo, and K. Papadopoulos (2012), Evidence for the oscillating two steam instability and spatial collapse of Langmuir waves in a solar type III radio burst, *Astrophys. J.*, *747*, L1.

Thornhill, S. G., and D. ter Haar (1978), Langmuir turbulence and modulational instability, *Phys. Rep.*, *43*, 43.

Walker, S. N., J. S. Pickett, D. A. Gurnett, and H. Alleyne (2003), High order spectral analysis of electron plasma oscillations in the electron foreshock, *Adv. Space Res.*, *32*, 309.

Zaitsev, V. V., N. A. Mityakov, and V. O. Rapoport (1972), A dynamic theory of type III solar radio bursts, *Sol. Phys.*, *24*, 444.
Zakharov, V. E. (1972), Collapse of Langmuir waves, *Sov. Phys. JETP*, *35*, 908.
Zakharov, V. E., S. L. Musher, and A. M. Rubenchik (1985), Hamiltonian approach to the description of non-linear plasma phenomena, *Phys. Rep.*, *129*, 285.
Zheleznyakov, V. V., and V. V. Zaitsev (1970), Contribution to the theory of type III solar radio bursts. I., *Sov. Astron.*, *14*, 47.

M. Bergamo and G. Thejappa, Department of Astronomy, University of Maryland, College Park, MD 20742, USA. (thejappa.golla@nasa.gov)
R. J. MacDowall, NASA Goddard Space Flight Center, Code 695, Greenbelt, MD 20771, USA.